J. Membrane Biol. 20, 13–30 (1975)

Ultraviolet Photoalteration of Ion Channels in Voltage-Clamped Lobster Giant Axons

G. S. Oxford and J. P. Pooler

Department of Physiology, Emory University, Atlanta, Georgia 30322

Received 31 May 1974; revised 28 August 1974

Summary. An analysis of the ultraviolet light-induced changes in ionic conductances of lobster giant axon membranes has been carried out using the double sucrose gap voltage-clamp technique. The predominant effect of monochromatic light from a xenon arc source in the 255 to 305 nm region is an irreversible reduction in the magnitude of sodium conductance, without change in sodium channel activation or inactivation kinetics. A considerably smaller reduction in the magnitude of potassium conductance occurs, with some slowing of potassium channel activation kinetics. Leakage conductance is essentially not altered. The fall in sodium conductance follows an exponential time course toward a zero asymptote. The rate constant for conductance decrease was used as an assay for the wavelength dependence. The sodium conductance was maximally sensitive at 290 nm. It is suggested that individual sodium channels are closed upon absorption of single photons by aromatic amino acid residues in membrane proteins.

A wide variety of techniques has been utilized by neurophysiologists to investigate the molecular events underlying the voltage-dependent conductance changes in excitable membranes. In addition to the ionic and pharmacologic approaches which have provided much useful information (*see* Hille, 1970, 1972), electromagnetic radiation has been employed both to probe the optical properties of normal membranes (Cohen, 1973) and to provide the initial energy to change membrane conductance properties (Pooler, 1972). The present work employs ultraviolet irradiation in this latter sense to alter excitable membranes of lobster giant axons to gain information relevant to the molecular basis for cellular excitation.

Studies of ultraviolet (UV) light alteration of nerve cells date back to Audiat in the early 1930's who first demonstrated action potential blockade during UV irradiation of frog sciatic nerve (Audiat, Auger & Fessard, 1931). Since that time several investigators have given consideration to the use of UV light as a tool for electrophysiological studies of the nerve membrane. Single unit studies on isolated frog nodes were initiated by Booth and co-

workers (Booth, von Muralt & Stämpfli, 1950) who found a threshold increase and a decrease in action potential amplitude without change in resting potential during UV irradiation. They proposed that the primary UV target was the sodium conductance system. Subsequent observations on single nerve fibers from other species, including squid (Gasteiger, 1953; Liudkovskaia & Kaiushin, 1960), crayfish (Gasteiger & Daube, 1962), earthworm (Bachofer, 1960), and crab (Lieberman, 1967) are consistent with a sodium pathway target. Confirmation of this target in the frog node was recently provided by Fox and Stämpfli (1971) who showed that sodium currents in voltage clamp fell during irradiation at 280 nm while significant changes in potassium current did not occur. These results demonstrate that some aspect of the voltage-dependent sodium conductance system in nerve membranes is UV sensitive and lead to the question as to which parameter or parameters are affected. The question also arises as to whether this UV sensitivity of the sodium system is found in all species, in view of the species dependent responses of nerves to certain pharmacologic agents and ions. For example, magnesium ions (Blaustein & Goldman, 1968), *Condylactis* toxin (Narahashi, Moore & Shapiro, 1969), tetraethylammonium ions (Armstrong & Hille, 1972), the insecticide DDT (Narahashi & Haas, 1968), or local anesthetics (Hille, 1970) may or may not exert a significant effect on a given conductance system depending on the preparation.

Action spectra often yield useful information concerning the identity of molecules participating in photochemically initiated processes. The present voltage clamp and optical system permit a precise determination of the action spectrum for the UV effect on ionic conductances. Thus, the aim of the present experiments is to (*i*) characterize the nature of the UV effect on ionic conductances of lobster axons, (*ii*) contrast the effect on lobster nerve with that previously reported for frog nodes, and (*iii*) obtain a precise action spectrum under voltage-clamp conditions.

Materials and Methods

Measurement and control of membrane current and voltage utilized the double sucrose gap technique (Julian, Moore & Goldman, 1962*a*, *b*). Single giant axons isolated from the circumesophageal connective of *Homarus americanus* were placed in a Lucite sucrose gap chamber with connection to the voltage-clamp electronic circuitry via Ag-AgCl electrodes in the external bathing solutions. There was no compensation for possible series resistance. Chilled artificial seawater (ASW) bathed the central pool axon membrane between the isosmotic sucrose flows. ASW contained ions in the following millimolar concentrations: Na^+ 428, K^+ 10, Mg^{++} 8, Ca^{++} 50, Cl^- 546, SO_4^{--} 4, HEPES (N-2-hydroxyethylpiperazine-N′-2-ethanesulfonic acid) 1. The pH was adjusted to 7.8. In several experiments ASW containing 10^{-6} M TTX was used to eliminate

sodium current. Central pool temperature was maintained at 3 to 6 °C as determined by a thermistor located near the solution outlet. UV irradiation of the submerged thermistor increased the temperature by less than 0.2 °C.

The optical system for UV irradiation incorporated a 1000 W high pressure xenon arc lamp (Hanovia model 976-Cl) mounted in a forced air ventilated aluminum housing (Electro Powerpacs model 371). The lamp output beam was focused via a quartz condenser onto the entrance slit of a $\frac{1}{4}$ meter Ebert-type grating monochromator (Jarrell-Ash model 82-410). The grating was blazed at 300 nm and etched at 2360 lines per mm resulting in a linear dispersion of 1.65 nm/mm in the plane of the exit slit. Both entrance and exit slits were 2 mm wide yielding an output bandwidth of 3.3 nm. Center wavelength was reproducible to within 0.2 nm using the digital wavelength readout. Calibration of the monochromator wavelength drive was accomplished with a mercury line source.

The monochromator output was collimated by a quartz lens and reflected at 45° by a MgF_2-coated aluminum front surface mirror (Microcoatings, Inc.) to a final quartz condenser which projected an image of the monochromator exit slit onto the axon membrane in the central pool. Intensity correction curves were generated from published output and transmission spectra of the optical components.

Voltage-clamp data was analyzed in terms of the parameters of the Hodgkin-Huxley model of excitation (Hodgkin & Huxley, 1952*b*). 35 mm film records of oscilloscope traces of membrane current and voltage were projected onto a grid and either traced onto graph paper or analyzed directly using a programmable desk calculator for the necessary computations. Leakage correction of total membrane current was accomplished by either of two methods. Sodium currents could be determined by subtracting records of total current before and after treatment with 10^{-6} M TTX. Alternatively, total current at time-to-peak inward current and steady-state outward current was leakage corrected by linearly extrapolating the currents from a standard 30 mV depolarizing prepulse at the corresponding times following the step to test potentials between -10 mV and the holding potential of -100 mV. For more positive test potentials the corresponding leakage current obtained at the sodium reversal potential, E_{Na}, where there is no sodium component was linearly extrapolated from the leakage value at -10 mV. The latter procedure attempted to correct for the rectifying component of leakage described previously (Pooler & Oxford, 1972).

Results

Action Potential Data

Ultraviolet irradiation at wavelengths between 280 and 290 nm produced drastic changes in electrically stimulated action potentials under current-clamp conditions. The example in Fig. 1 represents superimposed tracings of oscilloscope records of membrane action potentials taken at 30-sec intervals during continuous irradiation at 285 nm. A gradual decline in spike amplitude and maximum rate of rise is seen to occur which is initially unaccompanied by changes in the rate of repolarization or in the magnitude of measured resting potential. The threshold for excitation also increased during this time.

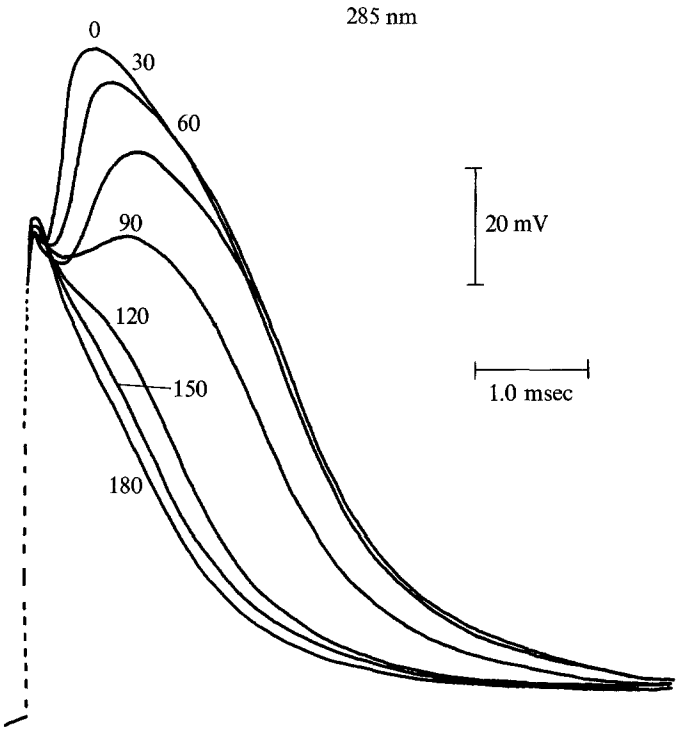

Fig. 1. Effect of UV on membrane action potential. Superimposed tracings of oscilloscope photographs of electrically stimulated action potentials. Numbers associated with each trace represent time of exposure to 285 nm light in seconds. A large amplitude stimulus was employed to ensure that firing would continue when irradiation increased the threshold

The observed changes in the size and shape of the action potential are similar to the effects of lowering the Na^+ concentration of the external bath or of adding TTX to the solution and suggest an involvement of the sodium ion pathway in the UV effect.

Voltage-Clamp Data

The effect of UV light upon membrane ionic currents under voltage-clamp conditions is illustrated in Fig. 2, where families of voltage-clamp currents are shown before and after 60 sec of exposure to 290 nm light. A marked suppression of the transient sodium current is seen to occur at all potentials. In contrast, changes in the magnitude of steady-state potassium current appear much smaller. Some slowing of the development of outward steady-state current is evident in this particular example.

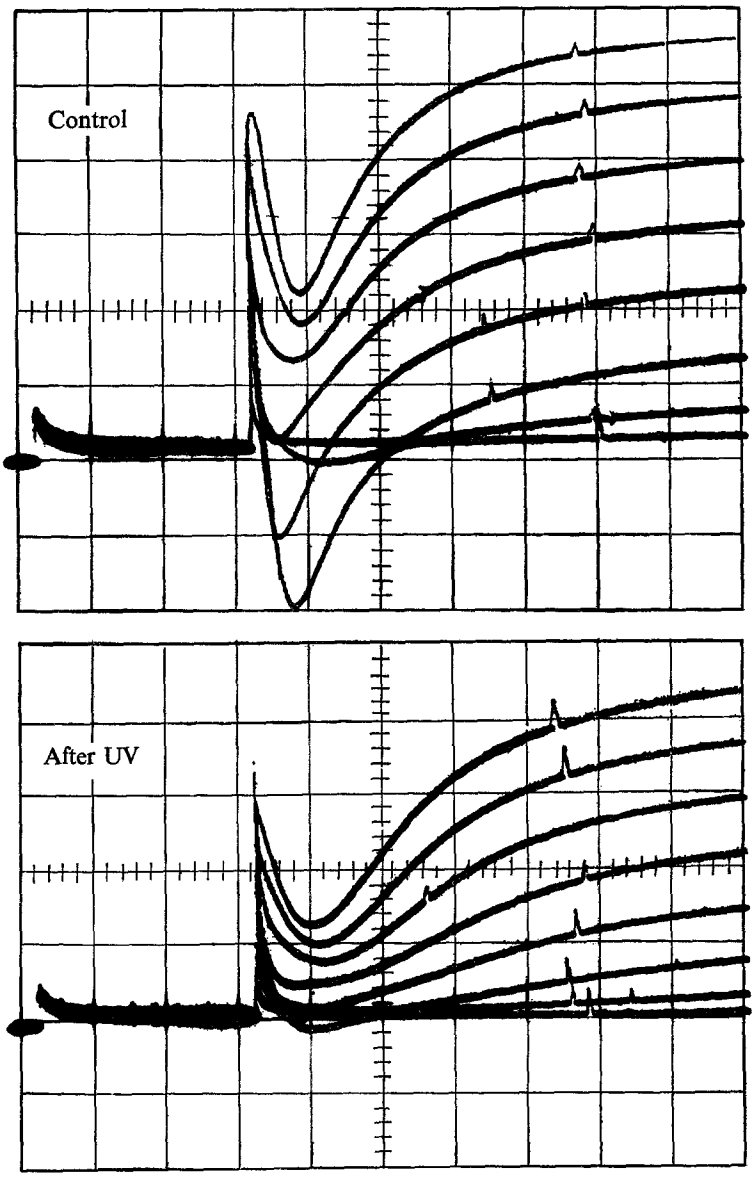

Fig. 2. Voltage-clamp current families before (upper half) and after (lower half) 1 min exposure to 290 nm light. Oscilloscope photographs of superimposed traces of membrane current in response to depolarizing steps between −60 mV and +80 mV in 20-mV increments. Each step is preceded by a 20-mV depolarizing prepulse. Holding potential of −100 mV. Grid scale represents 0.25 μA and 1 msec per division

Transient Sodium Current

The fall in sodium current during UV irradiation proceeds along an exponential time course towards an asymptote near zero. Fig. 3 is a plot of leakage-corrected peak sodium current measured every 10 sec during

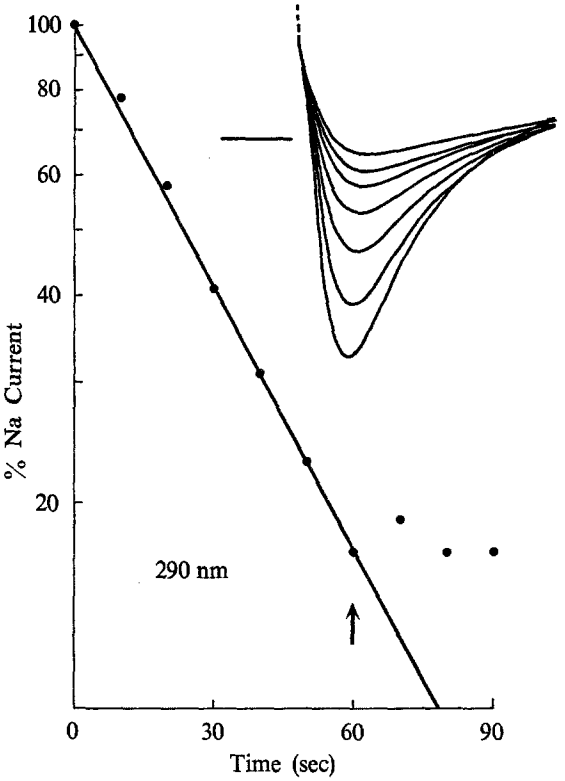

Fig. 3. Time course of sodium current decline during UV irradiation. Irradiation began at time = 0 and was terminated after 60 sec (arrow). Line drawn according to least-squares log regression fit to data points during UV exposure. Corresponding traces of transient current pattern are depicted to the upper right of the figure

290 nm irradiation. The line is drawn from a least-squares log regression fit to the data points during UV exposure (irradiation was terminated after 60 sec as indicated by the arrow). The rate constant for the decline of peak current during light obtained from the slope of the line is taken as an assay for the UV effect on the sodium system under varying conditions.

The corresponding current-time record is shown in the inset of Fig. 3. Time-to-peak sodium current is not altered, although time-to-peak *total* current increases slightly during illumination due to the progressively larger influence of the leakage time course at progressively smaller sodium currents. The absence of a change in time-to-peak sodium current suggests a lack of UV effect upon sodium channel activation or inactivation kinetics. This is supported by sodium "tail" experiments where the membrane was repolarized during maximum sodium conductance to a potential at which τ_m is expected to be large. The exponential time course of the decaying

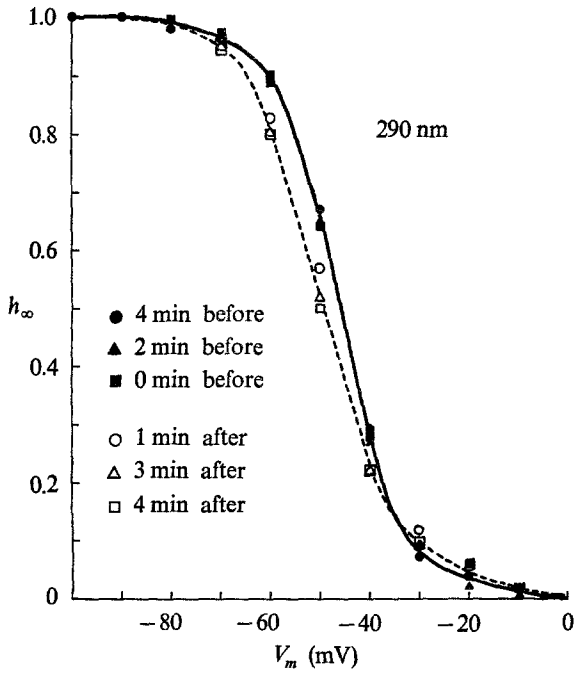

Fig. 4. Influence of UV upon steady-state sodium current inactivation. Filled symbols are data points for three identical voltage schedules before irradiation. Open symbols are data points on the same axon area following 1 min exposure at 290 nm. Data was leakage corrected by subtracting total current in each case from that observed in 10^{-6} M TTX. Smooth curves are drawn through data points before (solid line) and after (dashed line) UV

tail of current observed under this procedure was not altered during UV irradiation.

Steady-state sodium current inactivation was investigated using the double pulse technique (Hodgkin & Huxley, 1952*a*). The procedure involved repeating a test depolarization to 0 mV (a value on the positive limb of the I_{Na} *vs.* V_m relation) preceded in each instance by a prepulse of 50-msec duration and variable magnitude. The ratio I_{Na}/I_{Na_0}, where I_{Na_0} is the peak current during the test pulse in the absence of a prepulse, is taken as a measure of h_∞ at the end of the prepulse. h_∞ was plotted as a function of prepulse potential before and after 1-min exposures to UV light. Fig. 4 illustrates such a plot determined on an axon area for three identical prepulse schedules during a pre-UV control period and for three additional determinations following 60 sec of exposure at 290 nm. The data was leakage corrected by subtracting a set of currents obtained from the same voltage schedule after the addition of 10^{-6} M TTX to the bathing medium. Although irradiation reduced the magnitude of peak sodium current by 75%, the inactivation

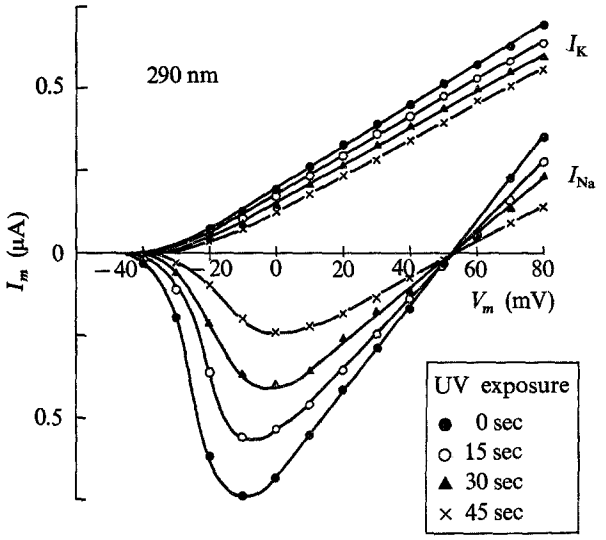

Fig. 5. Membrane current-voltage relations during irradiation. Peak sodium current (lower set of curves) and steady-state potassium current (upper set of curves) as a function of voltage are shown before and following three periods of UV exposure at 290 nm as indicated in the inset table

curve remained almost unchanged. There was a slight shift in the hyperpolarizing direction, averaging 1.7 mV in 19 determinations. A small decrease in slope of the curve was seen about half the time.

With a voltage-clamp system uncompensated for possible series resistance, the UV-induced reduction in sodium conductance could lead to slight shifts of the inactivation curve in the hyperpolarizing direction. (*See* Goldman & Schauf, 1972 for a discussion of this effect.) It is thus entirely possible that the small changes reported here are artifactual. At best the observed changes are minor and stand in contrast to the major effects on the sodium conductance magnitude.

Sodium current-voltage relations were examined at various stages of UV exposure as depicted in the example of Fig. 5. The sodium current is seen to decline during UV at all potentials investigated, both inward and outward sodium ion movement becoming increasingly restricted with increasing dose. The sodium current reversal potential, E_{Na}, remains constant during irradiation. The observed stability of the reversal potential under the present conditions suggests that the ion selectivity of remaining functional channels for sodium ions is not altered to a measurable degree.

A slight shift in the depolarizing direction of the potential where maximum inward current is obtained was observed and perhaps indicates a similar shift of the sodium activation parameter m_∞.

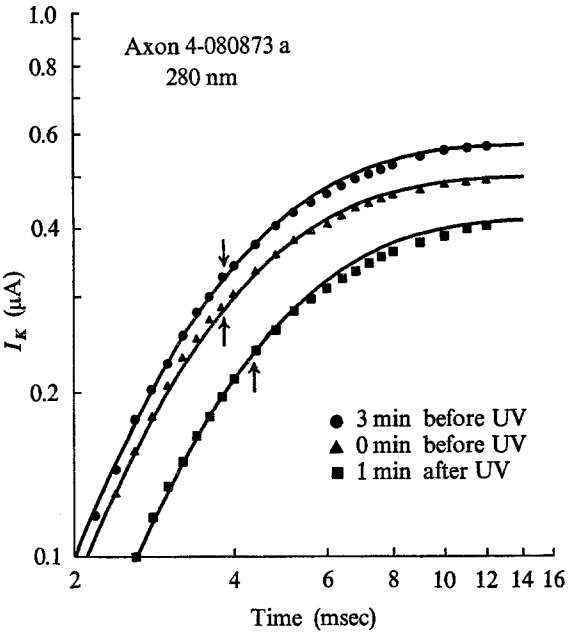

Fig. 6. Potassium currents during step depolarizations to +40 mV determined 3 min before (circles), immediately before (triangles) and immediately after (squares) 60 sec of UV. Lines drawn according to Eq. (1) where $x=4$. (*See text* for details)

Steady-State Potassium Current

Fig. 5 also illustrates the effect of 290 nm light upon the steady-state potassium current-voltage relation. The observed slope change in the potassium current-voltage curve is small, revealing the relative insensitivity of the delayed conductance to UV as compared to the transient g_{Na}. Possible changes in the value of the potassium current reversal potential are not observable from this data as E_K normally resides in a region of membrane potential where potassium channels remain closed.

In contrast to the absence of change in sodium current kinetics, the potassium current kinetics are observed to be somewhat slower following UV light treatment. Fig. 6 represents potassium current data from an axon area bathed in 10^{-6} M TTX seawater and step depolarized to +40 mV. The data is plotted in log-log format after Cole and Moore (1960) and the solid lines drawn according to Eq. (1)

$$I_K = I_\infty(1-e^{-t/\tau_n})^x \tag{1}$$

where I_∞ is the steady-state level of current, τ_n is the potassium activation time constant of the Hodgkin-Huxley model, and x is a dimensionless fitting

Table 1. Effect of ultraviolet light on potassium current kinetics

	$\tau_n(t_o)$	$\tau_n(t_f)$	$\Delta\tau_n(t_f - t_o)$
	1.7	2.2	0.5
	2.3	2.5	0.2
	1.9	2.3	0.4
	2.1	2.6	0.5
	2.1	2.45	0.45
	1.9	2.1	0.2
	2.2	2.35	0.15
	1.9	2.2	0.3
	1.9	2.15	0.25
	1.9	2.12	0.22
Mean ± SEM	1.99 ± 0.06	2.30 ± 0.05	0.32 ± 0.04
n	10	10	10

$p < 0.001$.
t_o = before UV; t_f = after 60 sec UV.

variable. During the 3-min control period a spontaneous decline in potassium current magnitude is evident but the kinetics are not changed. Following 60 sec of irradiation at 280 nm, however, the magnitude is further decreased and the kinetics are slowed, as shown by an increase in the value of τ_n during irradiation (marked by the arrows for each set of points).

The changes observed in τ_n at + 40 mV after 1-min exposures to 280 nm light are listed in Table 1 for several experimental areas. The average increase is small (16%), yet consistent, demonstrating a UV-induced change in potassium current kinetics.

Leakage Current

Leakage currents driven by 30-mV step depolarizations from a holding potential of − 100 mV were unaffected by 1.5-min irradiation periods at 280 or 290 nm. On some occasions, however, large depolarizations of TTX-treated axons to positive values of the membrane potential revealed slight decreases in leakage during irradiation. Owing to the complicated nature of leakage currents in sucrose gap (Pooler & Oxford, 1972) these effects at large depolarizations were not investigated systematically.

Reversibility

Experiments in which axon areas were alternately exposed to periods of UV irradiation and darkness demonstrated the photoalteration of

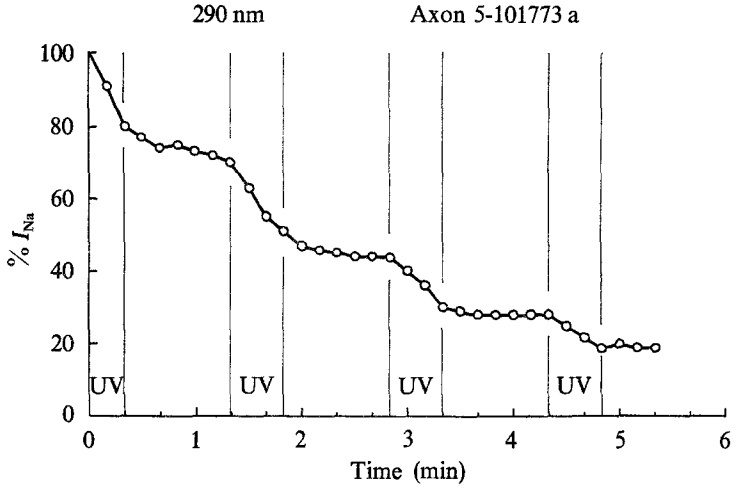

Fig. 7. Irreversibility of sodium current decline during UV. Peak sodium current during alternating periods of 290 nm irradiation and darkness

sodium channels to be irreversible. A typical experiment is depicted in Fig. 7, where peak transient sodium current measured at -10 mV decreases during the irradiation periods, but remains relatively constant during the intervening dark periods. Thus, during the time domain surveyed in these experiments a recovery of the sodium conductance toward initial levels was not observed.

The exponential nature of the photoinactivation of sodium conductance is again revealed as the current fell by approximately the same percentage for equivalent doses of radiation; the amount of current depressed being dependent only upon the amount of current remaining in each case.

Action Spectra

The sensitivity of the sodium channels to ultraviolet light is represented as a function of wavelength in Fig. 8 (open circles). The points are means ($\pm$ SEM) of the rate constants for the fall in sodium current during UV and are corrected for intensity differences. A major peak in the action spectrum occurs near 290 nm with a smaller maximum occurring at 265 nm. (The peak at 265 nm is relatively large due to the inclusion of one abnormally large rate constant, and is substantially reduced when the spectrum is based on the *median* rate constant values.)

The dashed line connects rate constant values for potassium current decline (filled circles). Spectral studies on the potassium conductance system

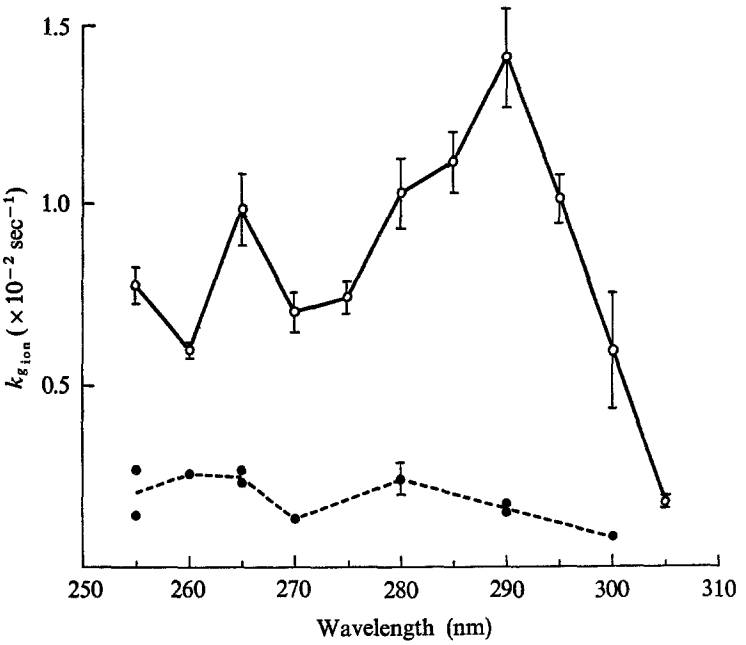

Fig. 8. Action spectra for sodium conductance (open circles, solid line) and potassium conductance (filled circles, dashed line). Means (± SEM) of rate constants for UV-induced fall in peak sodium or steady-state potassium current are plotted verses center wavelength of irradiation. From shorter to longer wavelengths, n for the sodium action spectrum was 3, 6, 5, 3, 8, 8, 7, 8, 4, 5 and 3. Individual rate constants are plotted for the potassium action spectrum except at 280 nm where $n=12$

were not extensive owing to the small magnitude of UV effect. It is clear from the data, however, that the potassium channel sensitivity never approached the sodium channel sensitivity at any of the wavelengths studied.

Much of the scatter in the rate constants of the sodium action spectrum results from appreciable axon-to-axon variation in overall UV sensitivity. The sucrose gap technique does, however, allow several independent measurements to be performed on separate areas of membrane from a single giant axon permitting spectral studies on one axon. The time course of sodium current decline at several wavelengths is shown as an example in Fig. 9 for a single axon and verifies the major peak in sensitivity to be near 290 nm.

Discussion

The data presented in this paper indicate that the alteration of membrane excitability induced by ultraviolet radiation of lobster axons is primarily a result of a progressive decrease in the maximum obtainable sodium con-

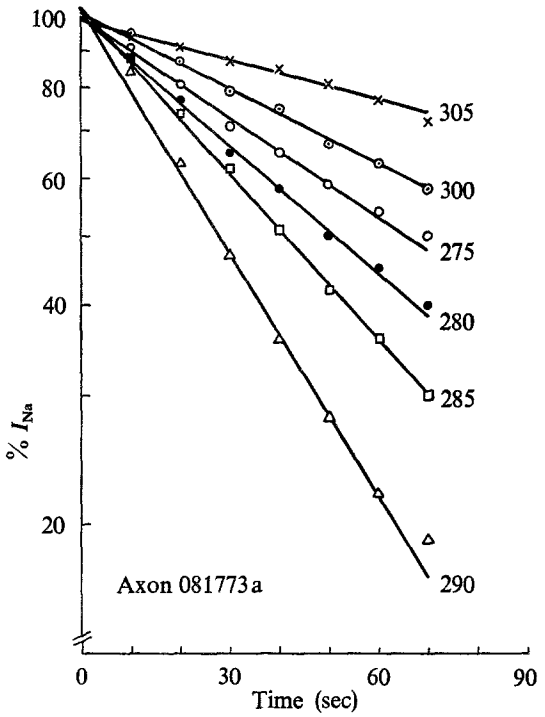

Fig. 9. Time course of UV-induced peak sodium current decline during step depolarizations to 0 mV at different wavelengths. Each determination was made on a separate experimental "node" of one single giant axon. Numbers associated with each set of points indicate irradiation center wavelength. Lines drawn according to log regression fits to data points

ductance, $\bar{g}_{Na}$. The maintenance of normal sodium current kinetics and the minimal effect upon the voltage dependency of sodium current after partial $\bar{g}_{Na}$ reduction indicate that the sodium channel gating properties remain essentially intact. Steady-state potassium conductance is much less sensitive to UV than the sodium conductance, although there does appear to be some small effect upon the potassium channel gating mechanism as revealed by a 16% increase in the average value of τ_n at +40 mV. While the measurement of leakage conductance under sucrose gap conditions is complicated by several factors, it does seem clear that the initial photoeffect is not simply a wholesale disruption of the axon membrane, as evidenced by the failure to observe any large increase or decrease in measured leakage current.

Our results confirm the data of Fox and Stämpfli (1971) who demonstrated a selective depression of the sodium current in nodes of Ranvier exposed to 280 nm light under voltage-clamp conditions. In the node of

Ranvier, as in the lobster axon, sodium channel kinetics remain unaltered and shifts of the sodium inactivation curve, when present, are very small and in the hyperpolarizing direction (Fox, 1972). Although quantitative information concerning UV effects on potassium current kinetics in the node of Ranvier are not yet available, it appears that if any changes do occur they are probably small (Fox, 1972). Thus, we conclude that the mechanism of excitability block is essentially identical in myelinated nerve fibers from *Rana* and giant axons from *Homarus*.

Much evidence has now accumulated supporting the idea that the sodium and potassium ions involved in excitation move across the nerve membrane at discrete loci referred to as channels and that sodium and potassium channels are independent and segregated on the basis of ionic selectivity, responses to certain drugs and toxins, and voltage response kinetics (*see* Hille, 1970; *see also* Armstrong *et al.*, 1973). The concept of individual sodium ion pathways is particularly attractive for interpreting the kinetics of the UV-induced fall in sodium conductance in terms of radiation target theory (Clayton, 1971). Target theory has been successfully applied to a variety of photoinactivation processes in other cellular and molecular systems.

If one assumes the fractional population of functional sodium channels to be directly proportional to the observed sodium current (at a constant maximum conductance per channel), the "survival curve" for sodium channels during UV irradiation is given by

$$N/N_o = 1-(1-e^{-kD})^m$$

where N is the number of remaining functional channels, N_o is the total number of channels (functional + blocked), D is the irradiation dose, k is a proportionality constant, and m is the target multiplicity or number of "hits" required to inactivate a single sodium channel.

If multiple sites per sodium channel must be altered by a photoreaction before ion passage through the channel is blocked ($m > 1$), the dose-effect curve will exhibit a "delay" at low doses of radiation and will approach a simple exponential at higher doses. Extrapolation of the exponential phase back to zero dose results in a vertical axis intercept of m, which gives a measure of the number of sensitive sites per channel. When $m = 1$ the dose-effect relation reduces to a simple exponential. This is the case for the data presented here (*see* Figs. 3 and 9) suggesting that the fall in sodium conductance during UV irradiation results from successive single photon-channel reactions progressively reducing the functional channel population.

The discrete channel model for sodium conductance provides for two ways of reducing $\bar{g}_{Na}$ – either a reduction in total channel number as mentioned or a reduction in the maximum conductance per channel. As a result, an alternative interpretation of the data would view the channel as possessing multiple sensitive sites, the inactivation of each site causing a constant fractional reduction in per-channel conductance. At present no convenient methods exist for distinguishing between the two mechanisms; however, as the former mechanism is attractively simple, the unnecessary complication of fractional channel conductance would seem to us to be unlikely.

With rare exception the action spectrum for a photo-induced phenomenon in biological systems parallels the absorption spectrum of the chromophore which initiates the event. Thus, the action spectrum for sodium current decline should offer strong evidence as to the identity of the chromophore associated with sodium channel photoinactivation. Maximum UV sensitivity in the lobster axon was found near 290 nm, falling off sharply at longer wavelengths.

It is possible that the action spectrum is artifactually shifted to longer wavelengths due to optical shielding by homarine, a substance found in considerable amounts in the cells of marine animals, including lobster and squid. Homarine absorbs maximally at 272 nm and probably accounts for the vast majority of the axon absorption in the wavelength range employed in these experiments (Eggen, 1957). A quantitative correction of the action spectrum for homarine shielding cannot be carried out because of lack of pertinent data. Hypothetical corrections, however, using various assumptions about Schwann cell thickness, optical path, etc., indicate that homarine shielding may have depressed the apparent axon sensitivity to wavelengths shorter than 290 nm, but not to the point of giving an erroneous value for the wavelength of peak sensitivity.

An action spectrum recently obtained for the sodium channel of the node of Ranvier by the same assay procedure is in general agreement with the one reported here (J. M. Fox, *personal communication*). Maximum sensitivity occurred at 280 nm with a very large contribution at 290 nm which again declines sharply for progressively longer wavelengths. Both spectra agree qualitatively with earlier action spectra based upon measurements of threshold increases in the node of Ranvier (Booth *et al.*, 1950) and action potential blockade in crab nerve fibers (Lieberman, 1967).

From a consideration of the absorption spectrum of lipids known to be in excitable membranes (Chacko, Goldman & Pennock, 1972) it seems unlikely that the lipid fraction makes a significant contribution to the UV effect. On the other hand, proteins show a characteristic peak in the 275 to

290 nm range due to the contribution of aromatic amino acid residues, particularly tyrosine and tryptophan (Wetlaufer, 1962). Such spectral coincidence with the action spectrum strongly suggests the involvement of one of these residues in the initial step of the photoinactivation of the sodium channel. This specific role does not, however, imply identity between the chromophoric element and the actual site where sodium ions pass through the channel. In this, as in other treatments which alter channels pharmacologically, the molecular site of action may be some distance from the site at which the membrane gates and selects ionic fluxes. The involvement of an aromatic amino acid in the photoprocess supports the widely held contention that the sodium channel is composed of protein. Surprisingly, additional evidence in support of this view is limited, the best perhaps relating specifically to the sodium inactivation mechanism (Armstrong *et al.*, 1973).

The participation of tyrosine and tryptophan in a variety of photoinactivation processes in enzyme systems is well documented (Vladimirov, Roshchupkin & Fesenko, 1970). These represent model systems potentially useful for the further investigation of the molecular basis for the UV alteration of the sodium channels in nerve membranes. Photon energy absorbed by aromatic residues in these systems can be dissipated by various pathways, the relative importance of each one depending on environmental conditions such as pH, pO_2, temperature, as well as the primary, secondary, and tertiary structure of the protein. Investigations to determine similar environmental dependencies of the sodium channel photoinactivation may serve to at least eliminate certain mechanisms as suspect in the phenomenon and perhaps to provide a partial picture of the functional relationships of molecules comprising the sodium channel.

This work was supported by NIH grant NS 09040.

References

Armstrong, C. M., Bezanilla, F., Rojas, E. 1973. Destruction of sodium conductance inactivation in squid axons perfused with pronase. *J. Gen. Physiol.* **62**:375

Armstrong, C. M., Hille, B. 1972. The inner quarternary ammonium ion receptor in potassium channels of the node of Ranvier. *J. Gen. Physiol.* **59**:388

Audiat, J., Auger, D., Fessard, A. 1931. Etude des courants d' action du nerf soumis au rayonnement ultra-violet. *Compt. Rend. Soc. Biol.* **107**:1218

Bachofer, C. S. 1960. Electrophysiological effects of ultraviolet radiation on single nerve fibers. *Arch. Biochem. Biophys.* **88**:333

Blaustein, M. P., Goldman, D. E. 1968. The action of certain polyvalent cations on the voltage-clamped lobster axon. *J. Gen. Physiol.* **51**:279

Booth, J. A., von Muralt, A., Stämpfli, R. 1950. The photochemical action of ultraviolet light on isolated single nerve fibers. *Helv. Physiol. Acta* **8**:110

Chacko, G. K., Goldman, D. E., Pennock, B. E. 1972. Composition and characterization of the lipids of garfish *(Lepisosteus osseus)* olfactory nerve, a tissue rich in axonal membrane. *Biochim. Biophys. Acta* **280**:1

Clayton, R. K. 1971. Light and Living Matter, Vol. 2: The Biological Part. McGraw-Hill, New York

Cohen, L. B. 1973. Changes in neuron structure during action potential propagation and synaptic transmission. *Physiol. Rev.* **53**:373

Cole, K. S., Moore, J. W. 1960. Potassium ion current in the squid giant axon: Dynamic characteristics. *Biophys. J.* **1**:1

Eggen, D. A. 1957. Some Ultraviolet Microspectrophotometric Measurements on Isolated Nerve Axons. Ph. D. Thesis. University of Chicago, Illinois

Fox, J. M. 1972. Veränderungen der spezifischen Ionenleitfähigkeiten der Nervenmembran durch Ultraviolette Strahlung. Ph. D. Thesis. University des Saarlandes, Germany

Fox, J. M., Stämpfli, R. 1971. Modification of ionic membrane currents of Ranvier nodes by uv-radiation under voltage clamp conditions. *Experientia* **15**:1289

Gasteiger, E. L. 1953. Effects of ultraviolet on electrical properties of invertebrate nerve. *Fed. Proc.* **12**:48

Gasteiger, E. L., Daube, J. R. 1962. A comparison of the effects of ultraviolet and ionizing radiations on electrical characteristics of nerves. *In:* Effects of Ionizing Radiation on the Nervous System. *Int. Atom. Energ. Agency Symp.*, Vienna

Goldman, L., Schauf, C. L. 1972. Inactivation of the sodium current in *Myxicola* giant axons. *J. Gen. Physiol.* **59**:659

Hille, B. 1970. Ionic channels in nerve membranes. *Prog. Biophys. Mol. Biol.* **21**:1

Hille, B. 1972. The permeability of the sodium channel to metal cations in myelinated nerve. *J. Gen. Physiol.* **59**:637

Hodgkin, A. L., Huxley, A. F. 1952*a*. The dual effect of membrane potential on sodium conductance in the giant axon of *Loligo*. *J. Physiol.* **116**:497

Hodgkin, A. L., Huxley, A. F. 1952*b*. A quantitative description of membrane current and its application to conduction and excitation in nerve. *J. Physiol.* **117**:500

Julian, F. J., Moore, J. W., Goldman, D. E. 1962*a*. Membrane potentials of the lobster giant axon obtained by use of the sucrose gap technique. *J. Gen. Physiol.* **45**:1195

Julian, F. J., Moore, J. W., Goldman, D. E. 1962*b*. Current-voltage relations in the lobster giant axon membrane under voltage clamp conditions. *J. Gen. Physiol.* **45**:1217

Lieberman, E. M. 1967. Structural and functional sites of action of ultraviolet radiations in crab nerve fibers. I. The electrophysiological effects of ultraviolet radiations. *Exp. Cell. Res.* **47**:489

Liudkovskaia, R. G., Kaiushin, L. P. 1960. Action of ultra-violet radiation on single nerve fibres. *Biophysics* **5**:38

Narahashi, T., Haas, H. G. 1968. Interaction of DDT with the components of lobster nerve membrane conductance. *J. Gen. Physiol.* **47**:965

Narahashi, T., Moore, J. W., Shapiro, B. I. 1969. Condylactis toxin. Interaction with nerve membrane ionic conductances. *Science* **163**:680

Pooler, J. P. 1972. Photodynamic alteration of sodium currents in lobster axons. *J. Gen. Physiol.* **60**:367

Pooler, J. P., Oxford, G. S. 1972. Low membrane resistance in sucrose gap—A parallel leakage path. *Biochim. Biophys. Acta* **285**:681

Vladimirov, Yu. A., Roshchupkin, D. I., Fesenko, E. E. 1970. Photochemical reactions in amino acid residues and inactivation of enzymes during U.V.-irradiation. A review. *Photochem. Photobiol.* **17**:9

Wetlaufer, D. B. 1962. Ultraviolet spectra of proteins and amino acids. *Advanc. Protein Chem.* **17**:303